THE EFFECT OF SLAB WARPAGE ON STRESSES AT CONTRACTION JOINTS

MICHIGAN DEPARTMENT OF STATE HIGHWAYS

THE EFFECT OF SLAB WARPAGE ON STRESSES AT CONTRACTION JOINTS

E. L. Marvin

Research Laboratory Section
Testing and Research Division
Research Project 39 F-1(8)
Research Report No. R-677.

State of Michigan
Department of State Highways
Lansing, August 1968

INFORMATION RETRIEVAL DATA

REFERENCE: Marvin, E. L., The Effect of Slab Warpage on Stresses at Contraction Joints, August 1968. Michigan Department of State Highways Research Report R-677. Research Project 39 F-1 (8).

ABSTRACT: Pavement slab warping, caused by temperature and/or moisture gradients, causes an upward (or downward) movement at contraction joints. This movement induces bending stresses in the dowel and causes the concrete above and below it to be deformed. The purpose of this study was to discover whether the stresses in the bar and slab would be large enough to cause plastic yielding of the dowel and compressive crushing of the concrete. Laboratory tests were conducted on concrete beams containing doweled open joints. These tests simulated the warping-induced joint face rotations that occur at pavement joints. The tests showed that a linear relationship exists between the change in bar curvature and the joint face rotation occurring at the joint. No quantitative measures of concrete bearing stress were obtainable from these tests. Extreme warping tests showed that the dowels used had less yielding strength than the supporting concrete mass. Data from these tests were compared with predictions based upon a mathematical model (elastic beam supported on one-dimensional elastic spring foundation). Data obtained indicate the model to be a good predictor of bar bending strain as a function of slab warping rotation. It is recommended that the probable warping stresses be considered in the design of doweled contraction joints.

KEY WORDS: bending stress, contraction joints, dowels, warping/concrete pavement/.

CONTENTS

THE EFFECT OF SLAB WARPAGE ON STRESSES AT CONTRACTION JOINTS

Pavement warping is caused by temperature or moisture gradients, or both, in the pavement slab. Warping occurs when a temperature gradient exists in the slab because the warmer side of the slab tends to expand relative to the colder side. Similarly, the damper portion of the slab tends to expand relative to the dryer side and causes warping when a moisture gradient exists. The resulting warpage can be concave with upward deflections occurring at the slab joints, or convex with downward deflections at the joints.

The magnitude and nature of these warping deflections have been investigated theoretically (1) and pavement warping deflections have been observed and measured on the MDSH US 27 test road (Research Project 47 F-13(1)). Observations of slab movement in the vicinity of contraction joints on the test road indicated that the slab actually lifted slightly off the base course in the vicinity of its joints. This upward deflection decreased to zero at a distance of 10 to 13 feet from the joint. The slope from the joint to the point of zero movement was found to vary from about 0.00083 to 0.002 in./in. Based on reference (1) for a slab with a free edge, the maximum theoretically predicted slope change due to slab warping would range from about 0.0013 to 0.0016 in./in.

Figure 1 shows the construction details of Michigan's concrete pavement contraction joints. Steel dowel bars, 1-1/4 in. in diameter by 18 in. long, extend through the joint and act as load-carrying devices that transfer live loads across the joint. These dowel bars are placed at 12-in. intervals transversely along the joint and are lubricated on one side of the joint with a cut-back asphalt coating. Due to temperature and shrinkage volume restraint a crack is formed (Fig. 1). During the winter months, contraction joints are found to be open as much as 1/2 in.; during the warm summer season the pavement slabs expand and the contraction joints are found to be nearly closed.

When upward warping occurs in the slabs on both sides of the joint simultaneously, the joint is lifted a small distance vertically and each joint face is rotated such that the joint is opened at the top and closed somewhat at the bottom. This movement of the contraction joint induces bending

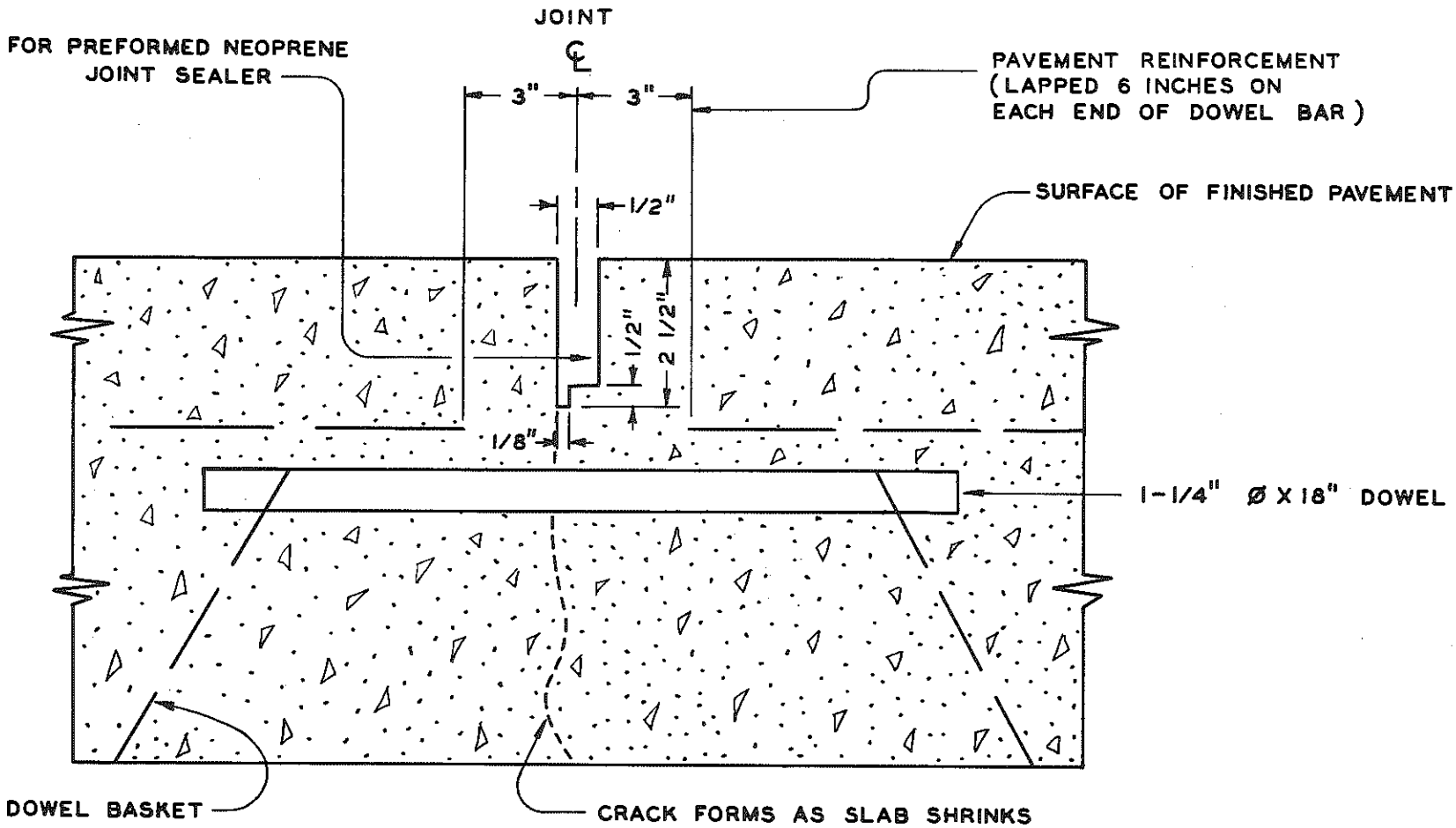

Figure 1. Transverse contraction joint details.

stresses in the dowel bars. The concrete in the region above and below each embedded bar is also deformed in constraining the bars. The rotation of the slab faces at the joint is less than that which would occur if the slabs had free ends. The rotation depends upon the deformation resistance of the concrete that supports the dowel bar, and the stiffness of the dowel in the open joint.

A preliminary analysis of the stresses in the bar and the slab that might be caused by warping deflections indicated that the stresses may be large enough to cause plastic yielding of the dowel bar and compressive crushing of the concrete. It was decided, therefore, to investigate the problem of slab warping-induced stresses in contraction joints under laboratory conditions.

The procedure adopted was to construct simulated contraction joints consisting of 9- by 12-in. concrete beams, 36 in. long, that contained instrumented dowel bars and open contraction joints. The beams were subjected to loading that induced rotations of the beam faces adjacent to the open joint. The joint face rotation and bar strain data from these tests were analyzed and the response of the test beams was compared with that predicted by a mathematical model.

SAMPLE CONSTRUCTION AND TESTING PROCEDURE

Four concrete beams (9 by 12 by 36 in.) were constructed--each with an open joint in the middle and a 1-1/4-in. diameter instrumented hollow dowel bar embedded in the beam, simulating a load transfer device. The dowel bars were constructed of steel mechanical tubing with an approximate yield strength of 60,000 psi. The moment of inertia of the hollow tubing was about 93 percent of that of a solid 1-1/4-in. diameter dowel of the type used in pavement contraction joints. Two strain gages were mounted in each bar at the center of the open joint. Details of the jointed beam specimen are shown in Figure 2.

The beams were mounted, one at a time, in the Laboratory's large test frame and loaded in bending across the joint portion of the beam as illustrated by the bending moment diagram in Figure 3. As the load was applied, the strains occurring in the top and bottom inside surfaces of the hollow dowel bar were measured by the strain gages located at the mid point of the joint.

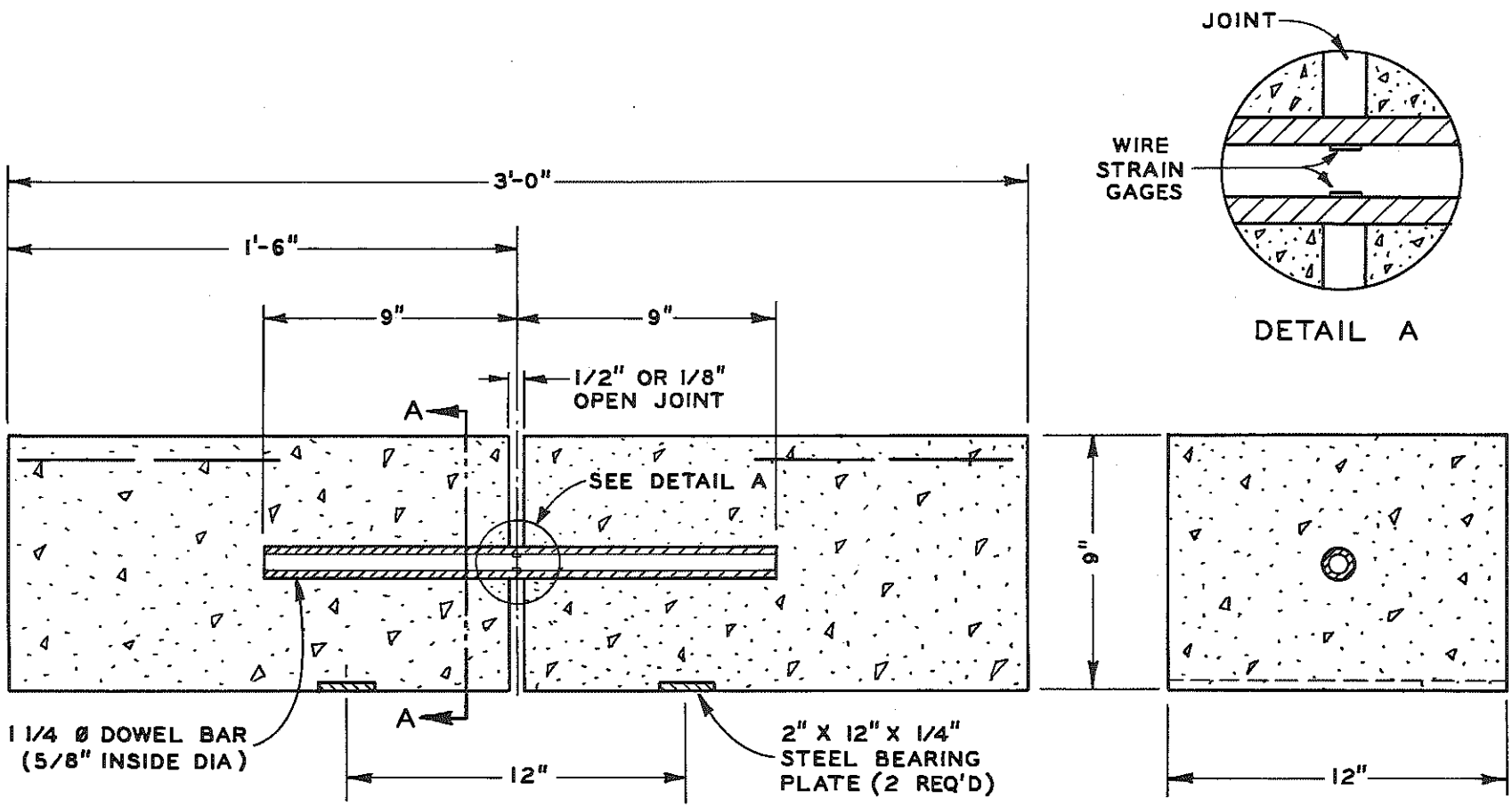

Figure 2. Details of jointed beam specimen.

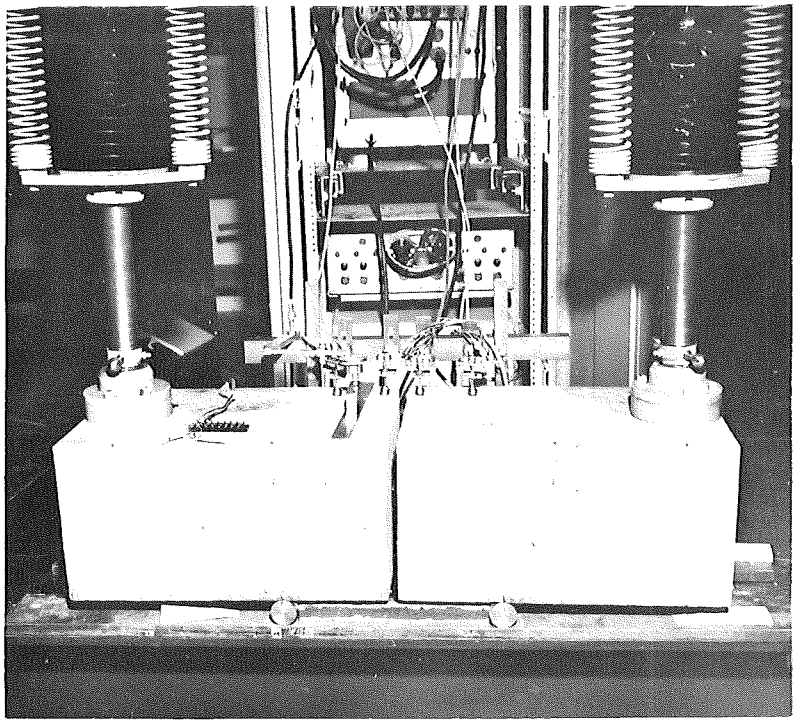

Beam being loaded in test frame.

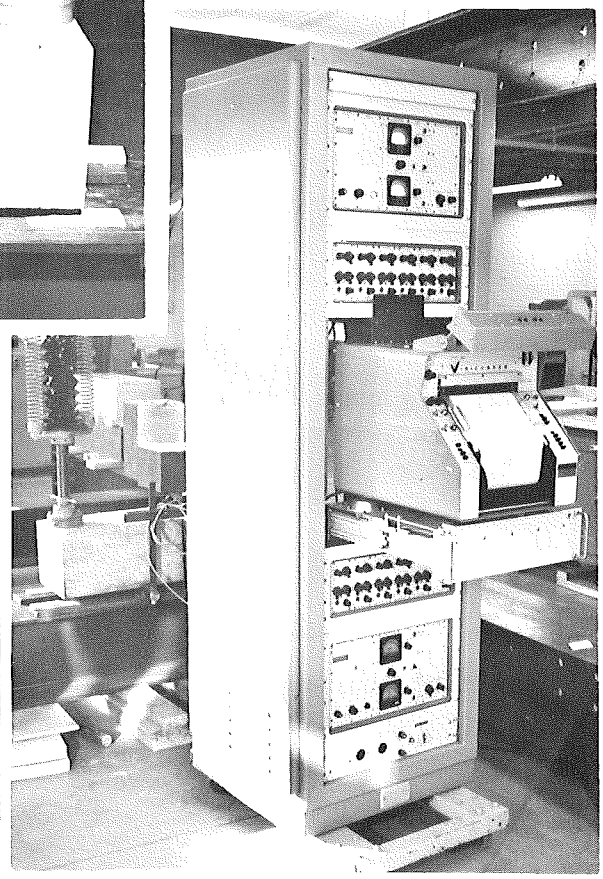

Continuous recordings were made of vertical movement and bar strain.

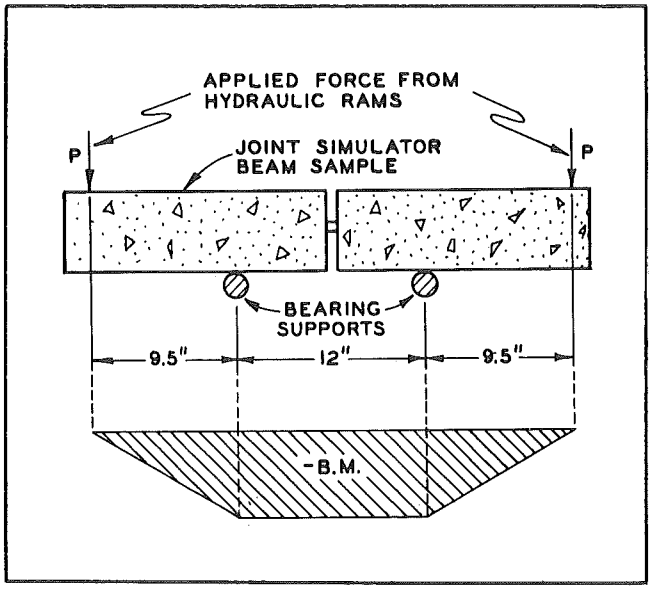

Bending moment diagram.

Figure 3. Warping test.

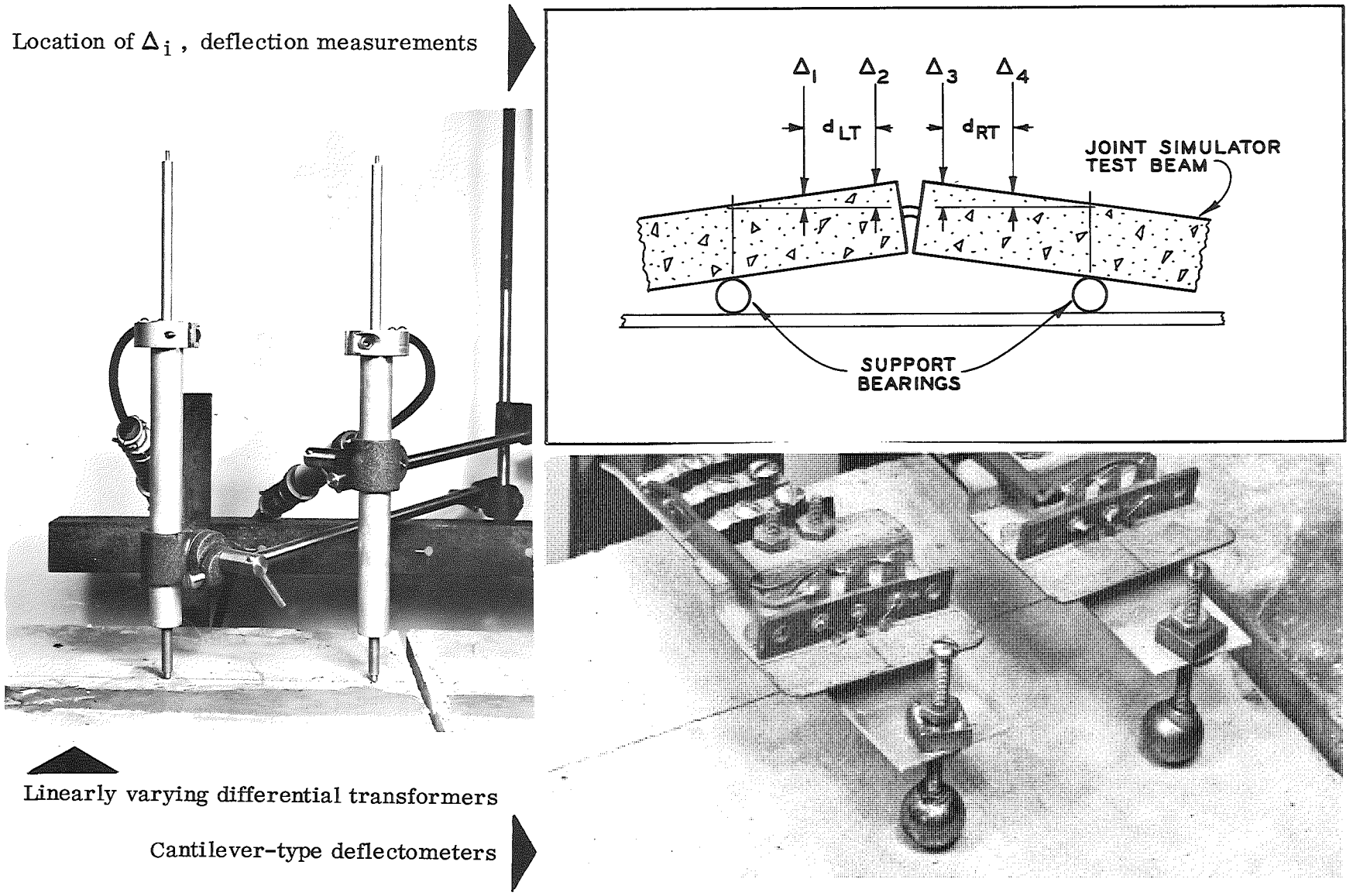

Figure 4. Beam deflection measurements.

As the loading proceeded, the joint rotated upward and the slope changed on the top surfaces of the beam adjacent to the open joint.[1] The vertical movement at the top surface was measured at four points as shown in Figure 4, where Δ_i denotes the measured upward deflection at points i = 1, 2, 3, or 4. Cantilever-type deflectometers were used to measure the vertical movements, in most of the warping experiments conducted. However, in a few tests, Linearly Variable Differential Transformers (LVDT) were used to measure the deflections (Fig. 4). The latter procedure was used in an effort to improve the method of measurement. The LVDT's performed better mechanically than cantilever-type deflectometers.

Using the measured deflections, the observed slope changes, θ_{Lt} and θ_{Rt}, near the left and right faces of the joint were computed using equations (1). Bar strain in the joint and beam surface deflections were measured and recorded throughout a first series of tests. The applied loads, P, were also recorded at predetermined points in the loading path.

$$(1) \qquad \theta_{Lt} \approx \tan\theta_{Lt} = \frac{(\Delta_2 - \Delta_1)}{d_{Lt}}, \quad \theta_{Rt} \approx \tan\theta_{Rt} = \frac{(\Delta_3 - \Delta_4)}{d_{Rt}}$$

where subscript Lt denotes left side and Rt denotes the right.

A second series of tests was conducted on one beam sample, using LVDT's to measure Δ_i. In one of these additional tests, the beam bending strains were measured at the surface of the concrete beam. The concrete beam strain data were used to determine how much the beams were bent in the vicinity of the joint.

TEST RESULTS

The warping tests performed in the laboratory were very limited in scope. Only four jointed beams were tested. Appendix A contains the analysis of these test results. The following conclusions are based upon the results of the limited testing performed:

1. The stresses that occur at a contraction joint when the joint faces are rotated by slab warping are significant. The warping tests on jointed

---

[1] The testing reported herein was confined to .002 in./in. slope change adjacent to the joint. This limit is equivalent to the maximum warping observed on the US 27 test road.

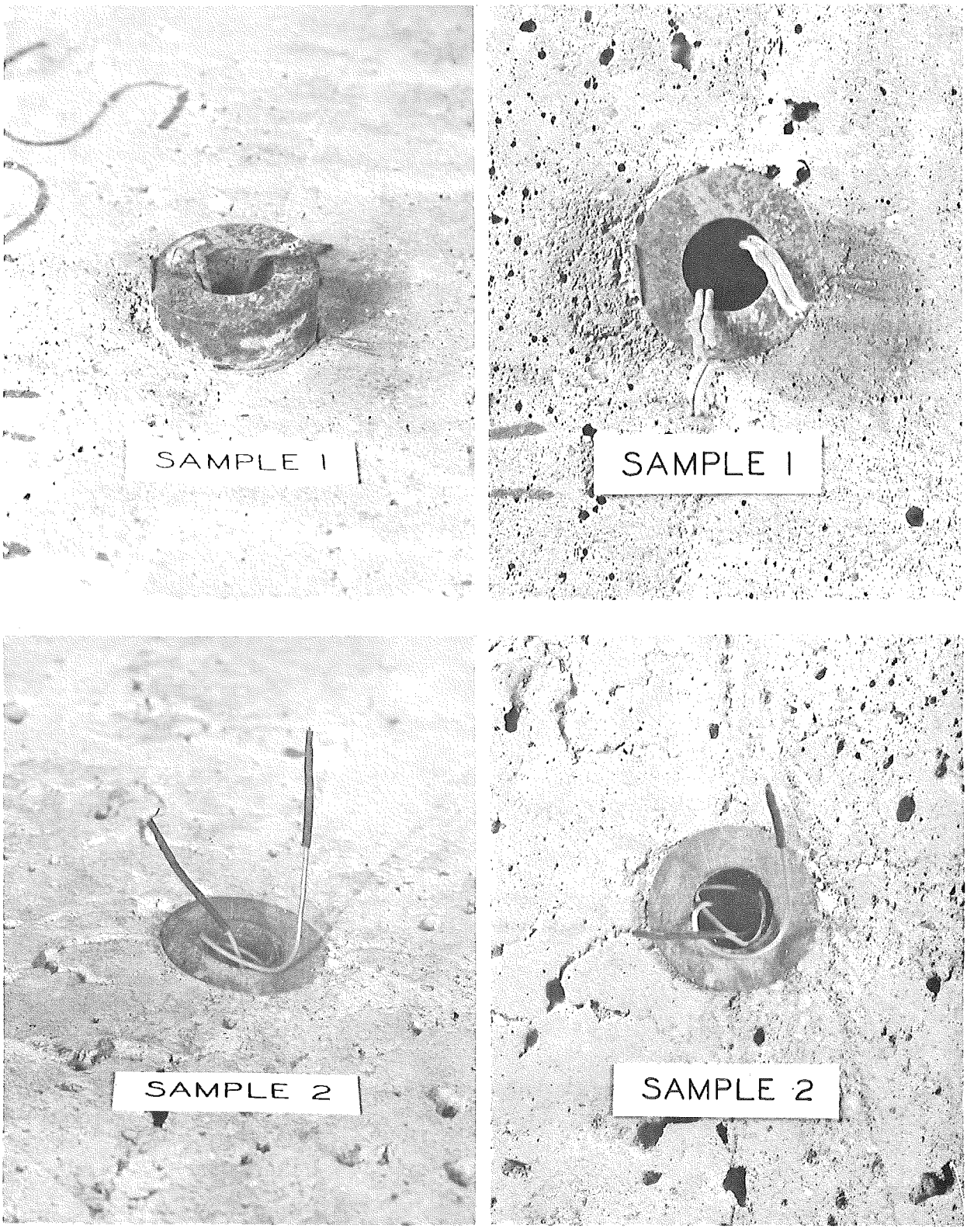

Figure 5. Photographs showing condition of concrete mass surrounding dowel bar after severe warping tests.

beams resulted in maximum dowel bar bending stresses of from 12,000 to 16,000 psi at joint face rotations equal to the maximum encountered on the US 27 test road. (These bar stress values were computed from measured bar strain.) The maximum bearing stress on the concrete below the bar at the face of the joint is estimated to have ranged from 450 to 1280 psi at joint face rotations of .002 in./in. in the tests conducted. (The bearing stresses obtained were not measured but were computed, using the elastic foundation theory as prepared by Friberg (3)).

2. The bearing stresses exerted by the dowel on the concrete, resulting from slab warping, are not of large enough magnitude to cause crushing of the concrete under the bar. This conclusion is based on the results of extreme warping tests (Fig. 5).

3. For joint face rotations less than .002 in./in., the joint warping tests showed that the rotations of the slab faces adjacent to a contraction joint are linear functions of the bar curvature change that occurs in the joint. This phenomena is exhibited in the θ versus $\frac{1}{R}$ plots of the warping test data (Fig. 6, Appendix A).

4. Attempts to determine β, a system parameter fundamental to the Friberg design theory (3), from direct concentrated loading tests such as reported in Appendix B-3 were unsuccessful. The reason for this is that the deflection of the dowel at the face of the concrete foundation appears to be a non-linear function of the load, if P is applied near the block face.

SUMMARY

Laboratory tests were conducted on concrete beams containing doweled open joints. The laboratory tests simulated the warping-induced joint face rotations that occur at pavement joints. (Joint face rotations of as much as .002 in./in. have been measured at existing pavement joints.) The tests showed that a linear relationship exists between the change in bar curvature and the joint face rotation occurring at the joint. Analysis of bar strain data from the warping tests showed that the maximum bar stresses that occur at .002 in./in. average joint face rotation are as much as 16,000 psi. No quantitative measures of concrete bearing stress were obtainable from the testing program. Extreme warping tests did illustrate, however, that the dowels used in this study had less yielding strength than the supporting concrete mass. At extreme warping deflections (as much as 30 times that known to occur at pavement joints), the dowel yielded plastically throughout

its cross section, whereas the concrete surrounding the bar at the face of the block did not show visible damage. (It is noted that the theoretical collapse loads of the hollow dowels were about 75 percent of that of solid 1-1/4-in. dia dowels).

The maximum concrete bearing stresses were estimated for .002 in./in. joint rotations from the bar strain data using the one-dimensional elastic foundation Friberg theory (3). The maximum concrete bearing stresses at .002 in./in. joint face rotation were computed to be as much as 1,280 psi. It is emphasized that the concrete bearing stresses obtained, using this theory, were not verified experimentally.

The determination of β , which is a system parameter used in the Friberg theory, by the direct loading of a dowel cantilevered from an embedding concrete mass was not found to be possible. In such tests performed, β was found to vary with load which was inconsistent with one-dimensional elastic foundation theory (Appendix B-3). An alternative procedure for approximating β is reported in Appendix B-2. The actual values of β used in computing bearing stresses were determined directly from the warping tests data.

It was concluded that slab warping induced stresses are significant and should be considered in the design of doweled contraction joints.

RECOMMENDATIONS

1. The stresses that are induced at contraction joints by slab warping should be considered in the design of pavement joints. It is recommended that the probable warping stresses be considered in the design of doweled contraction joints. The anticipated warping-induced stresses should be superimposed on the stresses that result from other design loads, and the total stresses should be limited to the allowable working stresses of the concrete pavement and steel dowels.

2. It is recommended that research be undertaken to provide a more theoretically sound method for computing the dowel bearing pressures.

APPENDIX A

ANALYSIS OF TEST RESULTS

Rotation of Slab Faces Adjacent to Joint

The data from the warping test on beam No. 2, which had a 1/8-in. open joint, are shown in Figure 6. At the top of that figure, a plot is shown of the observed joint face rotations that occurred on either side of the joint, versus measured bar curvature change in the joint. The graphs show that the relationships between the observed joint face rotations and the measured bar curvature change were approximately linear. However, the values of θ_{Lt} and θ_{Rt} at fixed values of $\frac{1}{R}$ were not equal. It is thought that this variation was caused primarily by rigid body rotations of the beam which took place as the loads were applied. (Analysis of the measured vertical movements, Δ_i, indicated that the beams rotated rigidly during the warping tests.) The effect of the rigid rotations can be eliminated from the data if the measured rotations of the left and right faces are averaged. This results from the fact that the rigid rotation increased θ on one side of the joint and decreased it on the other.

Rather than averaging each pair of θ values at each value of $\frac{1}{R}$, two straight lines were constructed which constituted least squares fits of the data from each side of the joint to a linear regression model. The slopes of the two lines obtained are denoted $\frac{d\theta_{Lt}}{d\left(\frac{1}{R}\right)}$ and $\frac{d\theta_{Rt}}{d\left(\frac{1}{R}\right)}$ in the figure. The rigid body rotation effect was eliminated by averaging the values of $\frac{d\theta_{Lt}}{d\left(\frac{1}{R}\right)}$ and $\frac{d\theta_{Rt}}{d\left(\frac{1}{R}\right)}$ obtained.

An analytical expression for $\frac{d\theta}{d\left(\frac{1}{R}\right)}$ is obtainable from the model equation (6) of Appendix B-1. The desired expression is obtained by differentiating

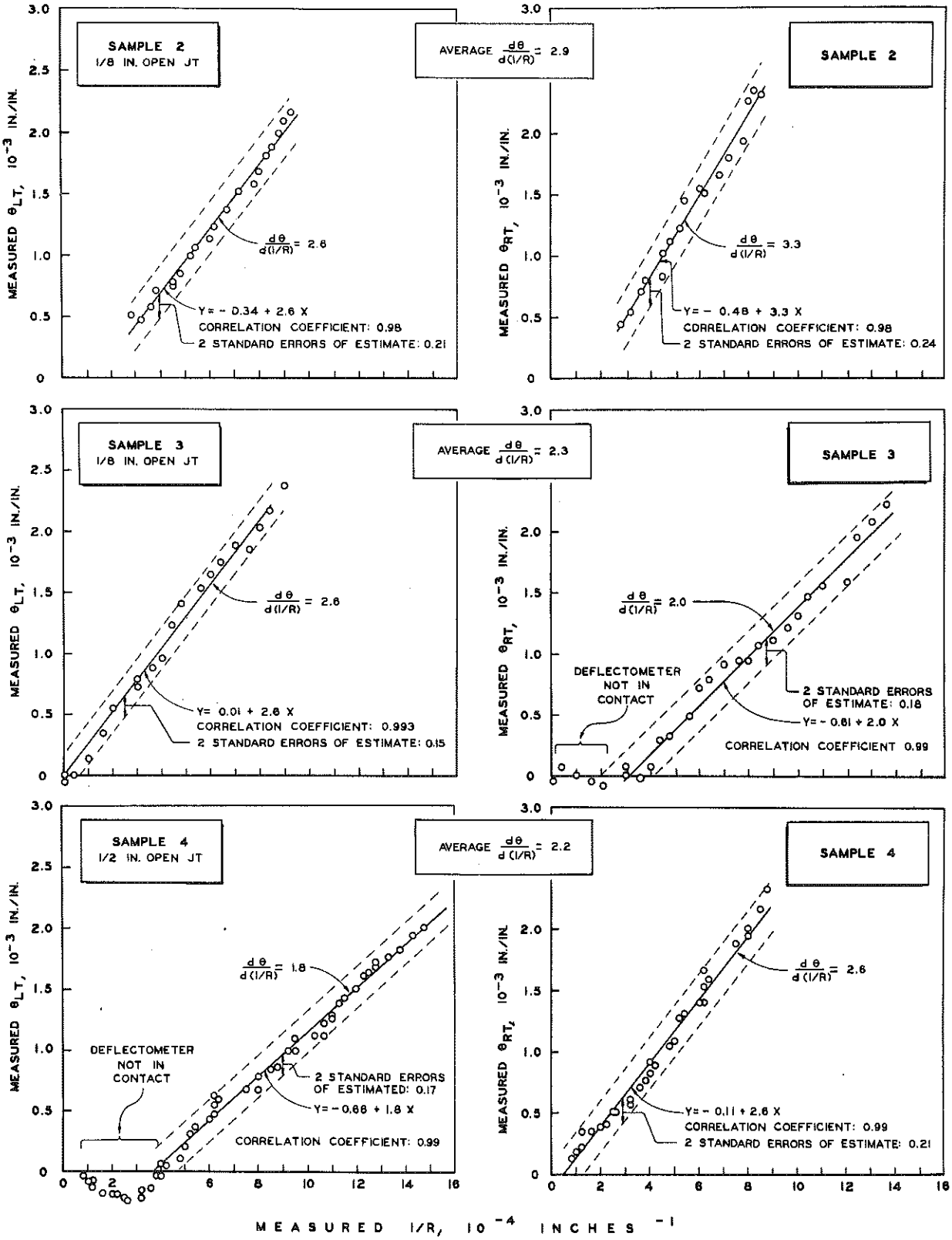

Figure 6. Data from warping tests on beams 2, 3, and 4.

equation (6) with respect to $\frac{1}{R}$. Expression (2) below, which was obtained

$$(2)\quad \frac{d\theta}{d\left(\frac{1}{R}\right)} = \frac{1}{\beta} + \frac{a}{2}$$

as indicated here, shows that according to the approximate theory used in this study, the average slope, $\frac{d\theta}{d\left(\frac{1}{R}\right)}$ obtained from Figure 6 should be equal to $\left(\frac{1}{\beta} + \frac{a}{2}\right)$. Conversely, the test results of this one experiment indicate that the constant β was equal to $\left(\frac{d\theta}{d\left(\frac{1}{R}\right)} - \frac{a}{2}\right)^{-1} = .35$ for test beam 2.

Data from warping tests on beams 3 and 4 are also shown in Figure 6. The plots show that the slab faces rotated as linear functions of measured curvature in the tests on these other beams also. Table 1 summarizes the results of the original tests on beams 2, 3 and 4. The apparent values of β obtained from the warping tests on jointed beams are given in Column 4 of the table.

Additional evidence of the existence of a linear relationship between the joint face rotations and $\frac{1}{R}$ in the joint was obtained in further testing performed on beam No. 3. Five additional warping tests were conducted in which the deflections were measured on one side of the joint only, using LVDTs instead of cantilever deflectometers. In these six tests, the θ versus $\frac{1}{R}$ data also fell along straight lines.

Stresses at the Joint

The stresses in the bar due to bending that occurred in these warping experiments can be calculated from the measured bar strain data. (Strain was converted to bar curvature, $\frac{1}{R}$, for presentation in Figure 6.) The stresses that occurred at .002 in./in. average joint face rotation are required since that value is equivalent to the maximum value observed on the

test road. In order to estimate what the curvature was at .002 in./in. average joint face rotation for each test, it was assumed that all of the θ versus $\frac{1}{R}$ relationships shown in Figure 6 should have passed through the origins of the graphs. This was done because there is no reason to believe that strain should have occurred in bars without any change in joint face rotation.[1] The curvature of the bars at .002 in./in. average joint face rotation was determined by integrating the constant values of $\frac{d\theta}{d\left(\frac{1}{R}\right)}$ given in Column 5 of Table 1, solving the resulting equation for $\frac{1}{R}$ using the initial condition $\frac{1}{R} = 0$ at $\theta = 0$, and evaluating the expression obtained for $\frac{1}{R}$ at $\theta =$ .002 in./in. The values of $\frac{1}{R}$ that were determined are given in Column 6 of Table 1.

TABLE 1
JOINT STRESSES AT .002 IN./IN. JOINT WARPING ROTATIONS

Beam No.	Run No.	Joint Width, in.	β	$\frac{d\theta}{d\left(\frac{1}{R}\right)}$	$\frac{1}{R}$ [1] (in^{-1})	Max. Bar[2] Stress in Joint, psi	Bearing Stress[2] Under Bar at Joint Face, psi
2	1	.12	.35	2.9	6.9×10^{-4}	12,500	450
3	2	.12	.45	2.3	8.7×10^{-4}	15,700	920
4	1	.54	.52	2.2	9.1×10^{-4}	16,400	1280

NOTE: [1] $\frac{1}{R} = \left(\frac{.002}{\frac{d\theta}{d\left(\frac{1}{R}\right)}}\right)$

[2] $E_s = 29 \times 10^6$

The bar stress at the outer fiber of each bar, the maximum stress, was then calculated using the first equation (7) from Appendix B-1. The

[1] The offsets along the $\frac{1}{R}$ axes of the straight line functions on the graphs in Figure 6 were caused by inaccurate determinations of the initial zero strain level on the oscillograph records of the data and an initial lack of deflectometer contact with the beams in some experiments.

maximum bar stresses that occurred in each of the beam joints at .002 in./in. average joint face rotation according to this procedure are shown in Column 7 of Table 1. It can be seen that the magnitudes of the bar stresses were significantly large at .002 in./in. warping.

Knowing the $\frac{1}{R}$ values at .002 in./in. warping, it is also possible to estimate the maximum bearing stresses that occurred under the bars at concrete beam faces in the experiments if the elastic foundation theory as applied by Friberg (3) is assumed valid. These computations were performed by substituting known $\frac{1}{R}$ values in Equation (9) of Appendix B-1. The estimated values of the maximum bearing stresses that occurred at .002 in./in. average joint face rotation are shown in Column 8 of Table 1. These estimates indicate that the maximum concrete bearing stresses resulting from slab warping were significantly large also. It is emphasized, however, that these bearing stresses were computed using an approximate foundation theory and are not based on measured concrete strains.

Extreme Warping Tests

Test beam sample 1, which has a .5-in open joint, was subjected to a severe warping test. In the test, an attempt was made to load the beam to failure. The loading was continued until the bottom of the joint closed completely. This was equivalent to an observed joint face slope change of approximately 0.06, or 30 times the maximum slope change observed on the US 27 test road. Since the dowel bar appeared to be yielding plastically, it was decided to discontinue the test. After the beam was unloaded, a permanent slope change was noted. The top of the joint remained open 7/8 in. and the bottom was open 5/32 in.

The bar was then cut through in the open joint, separating the beam into two blocks. It was apparent from visual inspection that no major crushing of the concrete had occurred. In fact, the concrete appeared undisturbed in the region surrounding the bar (Fig. 5).

The theoretical collapse loads of the hollow dowels used in these experiments were about 75 percent of the collapse values of solid 1-1/4-in. diameter dowels of the type used in pavement contraction joints[2]. Although

---

[2] Collapse load is defined as the bending load at which the plastically deformed region of the bar extends throughout the transverse bar cross-section.

the dowel used in the experiment was somewhat weaker than solid dowels used in pavement joints, the results obtained are quite significant because the magnitude of the warping rotations induced in the experiment was much larger than that which actually occurs at pavement joints in service.

The severe test performed on Sample 1 illustrated qualitatively that the dowel bar had less ultimate yield strength than the concrete mass surrounding it at the joint. This indicated that .002 in./in. warping of real pavement joints should not cause gross concrete failures around the dowels.

Test beam 2 was also subjected to an extreme warping test. After completing the normal warping test in which loads of about 700 lbs were applied by each cylinder, as illustrated in Figure 3, the loading was continued to 3400 lbs. After the loads were removed, a residual warpage at the joint was noted, indicating plastic yielding of the bar. Visual examination of the beam faces that are shown in Figure 5 revealed that the concrete surrounding the bar had not been damaged in the test.

APPENDIX B-1

THEORY OF JOINT RESPONSE

For the purpose of this analysis, it was assumed that concrete responds to load in a perfectly elastic manner. This assumption is based on the fact that the stresses, strains, and strain rates encountered in this study have all been small.

The mathematical model of joint warping response that will be discussed here neglects the possibility of dowel bar slippage. Since one end of the dowel bar is lubricated, it seems possible that some slip might occur between the concrete and the outer bar surface. Very little slip was observed in the laboratory tests, however, and therefore it does not seem necessary to provide for joint slip in the model theory.

Considering the contraction joint's mechanical response to warping in a qualitative way, it is apparent that the joint reacts to warping forced rotations of its faces in three ways. As the joint is warped upward (or downward), the following reactive phenomena occur:

1. The dowel bar is bent in the open joint.

2. The concrete that embeds the dowel is deformed as the dowel bends within the concrete mass.

3. The concrete slab as a whole is bent slightly downward by the resisting dowels as the joint is warped upward (or bent upward if the warping is downward).

In order to devise a mathematical expression that will predict the deformation that will occur at the joint when warping occurs, it is necessary to relate the three listed reactive phenomena to warping-induced joint face rotations, quantitatively. To do this, each of the three phenomena will be analyzed separately for a constant warping condition. The resulting expressions relating each of the three reactive features to warping will then be superimposed. Finally, the total superimposed expression will be assumed valid for a range of warping rotations.

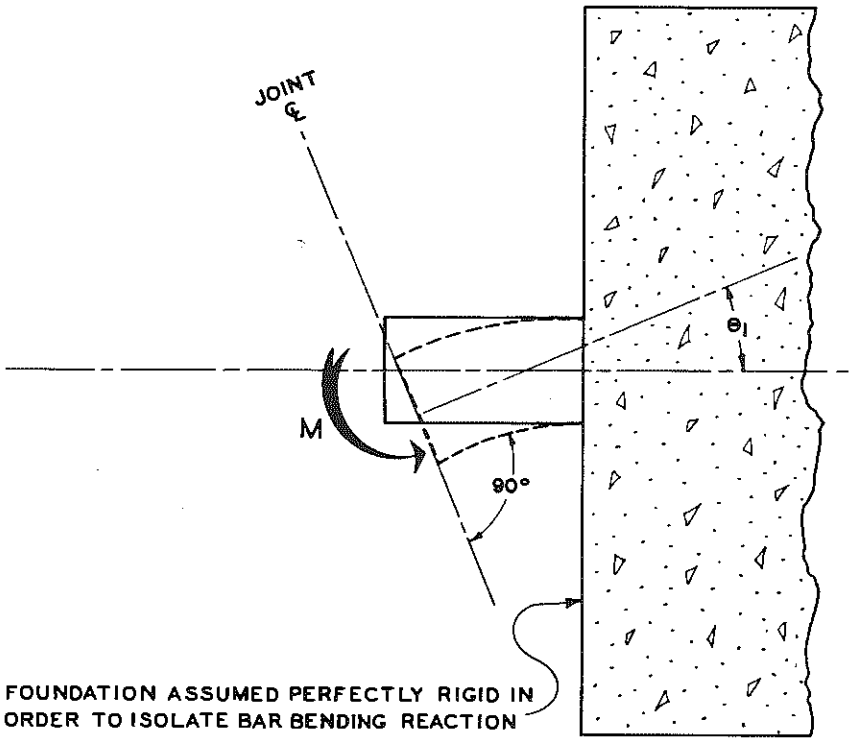

Figure 7. Rotation, θ_1, attributable to bar bending in joint.

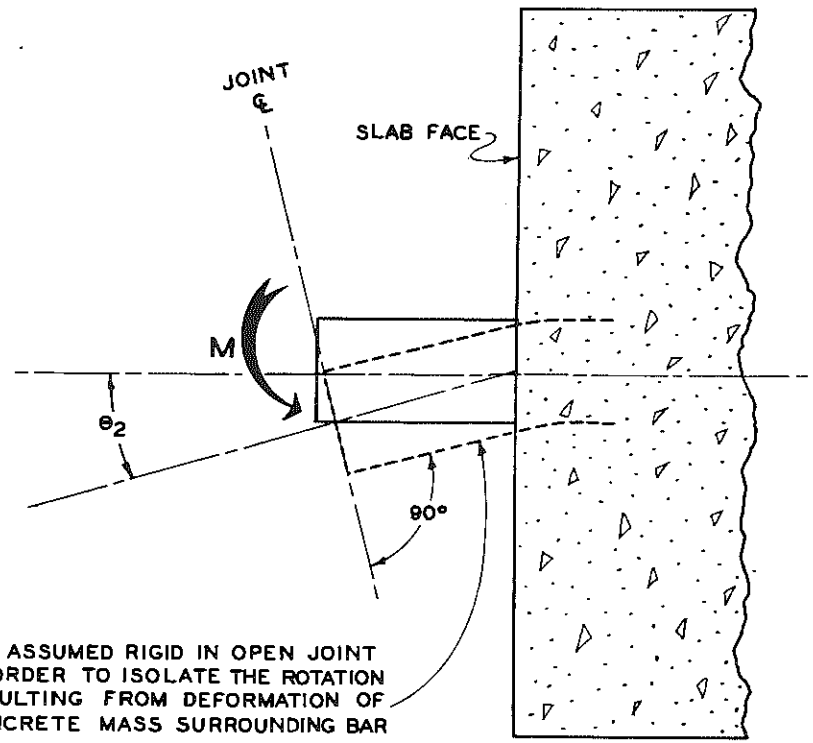

Figure 8. Rotation, θ_2, attributable to deformation of embedding concrete mass.

Mathematical Model Construction

1. Bar Bending Resistance

The curvature that is induced in the dowel bar by the warpage causes the bar to deform as an elastic beam in the open portion of the joint. Figure 7 shows that as the bar bends in a circular arc away from its original axis, it forms an angle θ_1, between the tangent to the deformed axis of the bar at the midpoint of the joint, and the original axis.

Equation 1, below, gives the magnitude of θ_1. (This formula was derived by treating the bar as a beam subjected to a uniform bending moment.)

$$(1) \quad \theta_1 \approx \frac{a}{2R} = \frac{a\,M_o}{2\,E_s I}$$

where:

M_o	=	Bending moment developed in the bar
a	=	Joint opening
E_s	=	Young's modulus of elasticity of steel dowels
R	=	Radius of curvature of deformed bar in the open joint
I	=	Moment of Inertia of bar

2. Foundation Deformation--Elastic beam supported on an elastic foundation.

As the joint warps upward, the dowel deforms the concrete that supports it. This deformation allows the bar to deflect in the concrete mass and rotate at the face of the joint as shown in Figure 8. The right angle which existed between the axis of the bar and the face of the joint prior to the deformation is increased by the angle θ_2. This deformation process is similar to that described by an ideal elastic beam of infinite length supported on an elastic foundation. The deflection of an elastic beam supported on an elastic foundation has been approximated by Timoshenko (2) and the actual problem of a dowel bar embedded in a concrete pavement joint has been treated by Friberg (3). According to this approximate theory, the dowel deflects on a simplified spring foundation as shown in Figure 9. (The elastic solid support is replaced by a series of springs.) When bending

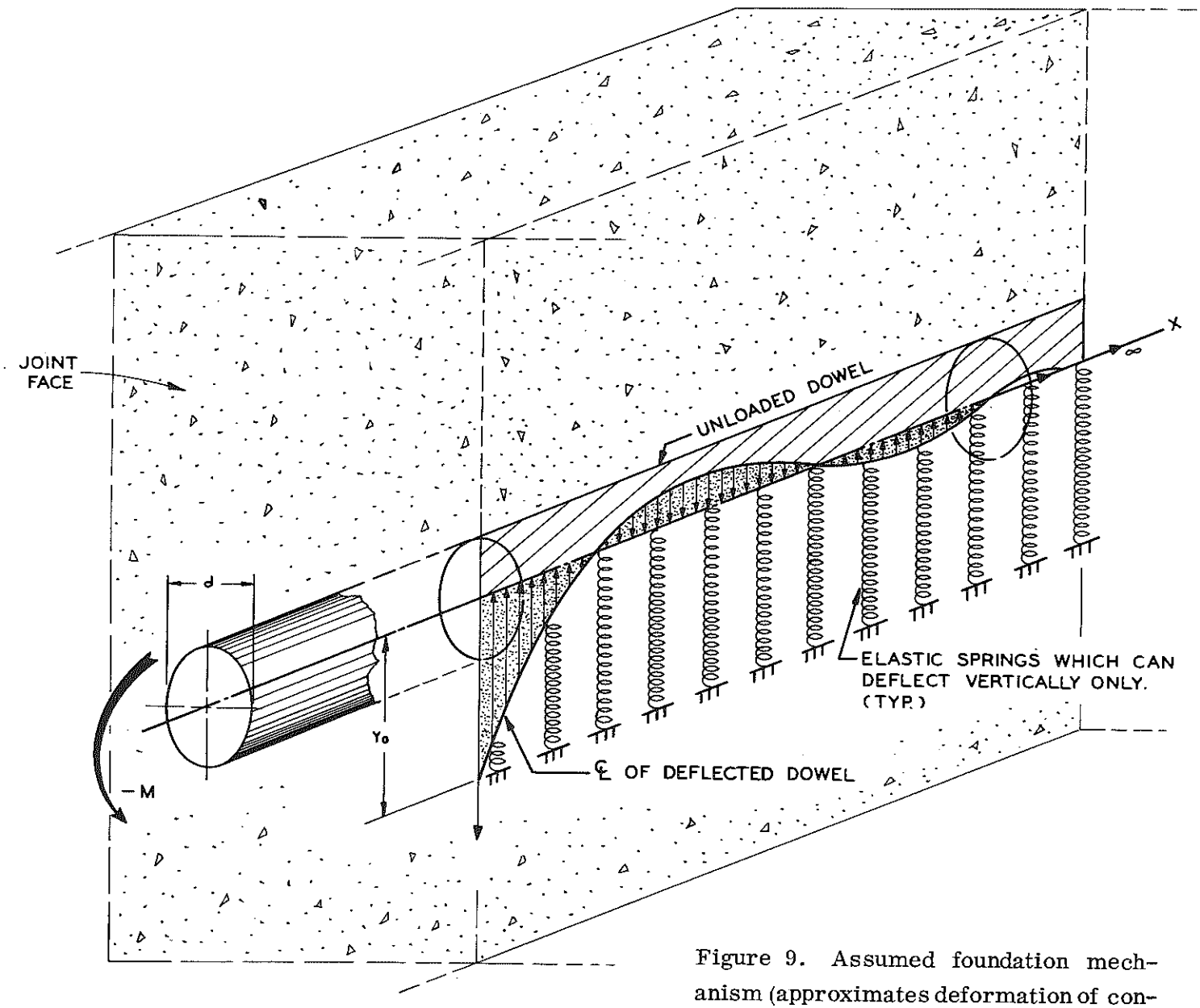

Figure 9. Assumed foundation mechanism (approximates deformation of concrete mass surrounding bar.)

moment M_o is applied to the bar, the springs that are assumed to support the embedded bar respond, and are deformed elastically. Using the expression for the slope of the beam deflection curve given in reference (3), the angle θ_2, can be expressed in terms of M_o. If the bending moment, M_o, is known θ_2 can be computed using equation (2) which is the $\theta = \theta\ (M_o)$ expression derived from reference (3)

$$(2)\quad \theta_2 \approx \left.\frac{dy}{dx}\right|_{x=o} = \frac{M_o}{\beta\ E_s I} = \frac{1}{\beta\ R}$$

where: M_o = Bending moment applied at the face of the foundation, at x = o

E_s = Modulus of elasticity of steel bar (beam)

I = Moment of Inertia of bar

R = Radius of curvature of bar at face of joint

$\beta = \left(\frac{Gd}{4E_s I}\right)^{\frac{1}{4}}$

G = Modulus of support of the concrete mass

d = Outside diameter of bar

3. Bending of Foundation

Figure 10 illustrates how the slab is also bent when a bending moment, M_o, is developed at the joint. The slope change θ_3 is opposite in sign to θ_1 and θ_2. Equation (3) gives the slab bending slope change, θ_3, in terms of the measured radius of curvature of the concrete slab adjacent to the joint.

$$(3)\quad \theta_3 \approx \frac{L}{R_c}$$

where: L = Unsupported length of beam or slab

R_c = Radius of curvature of concrete beam or slab

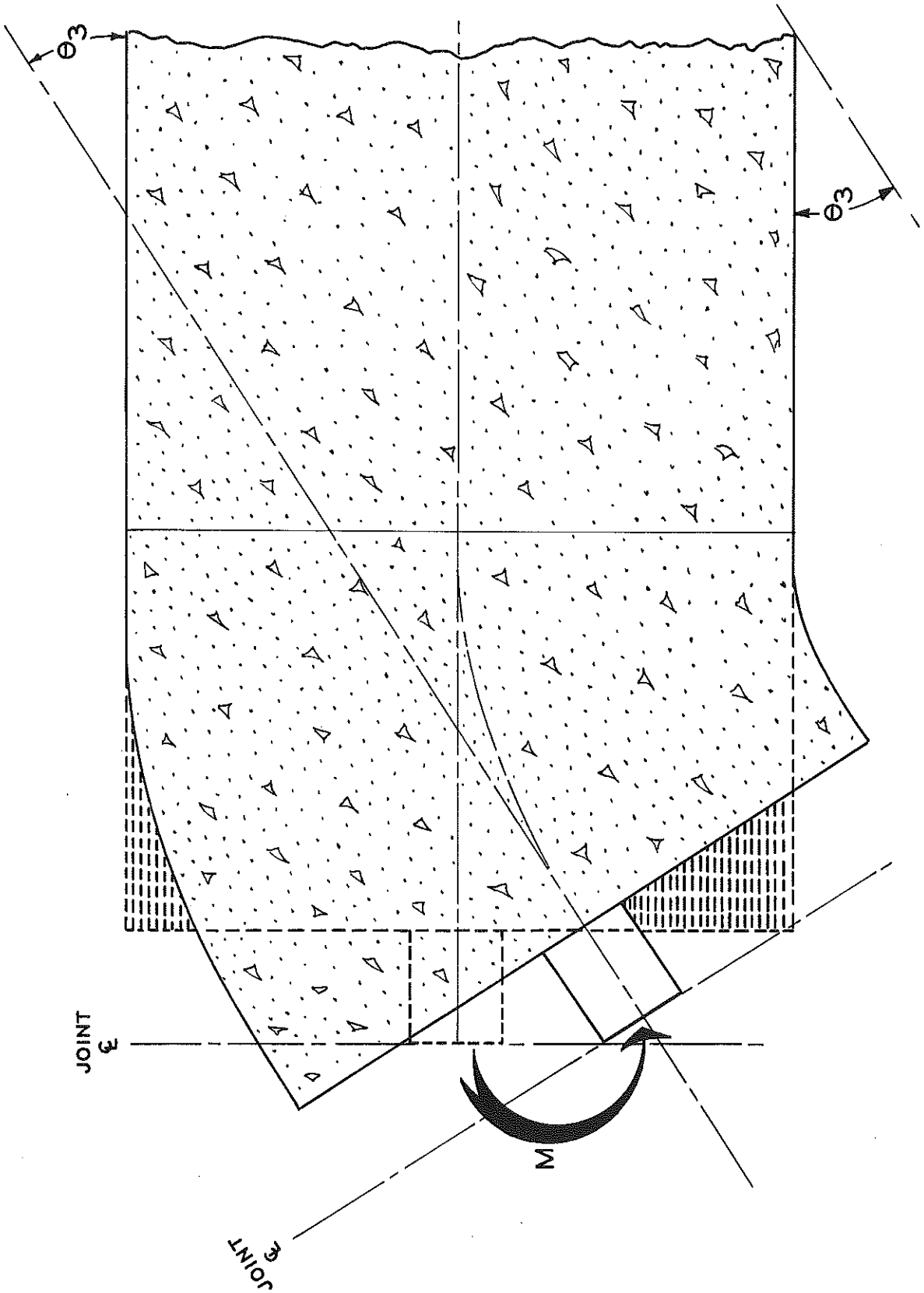

Figure 10. Slope change caused by bending of slabs or beam.

4. Bending of Elastic Beam on Bending Elastic Foundation (Superposition of the three reactive phenomena).

In order to mathematically describe the slope changes that can be expected to occur in the concrete slab adjacent to a contraction joint due to slab warping, the three mechanisms of slope change response (θ_1, θ_2, θ_3) must be combined. In order to do this, the observable slope change at the joint in a beam, or slab, is assumed to be equal to the algebraic sum of θ_1 , θ_2 , and θ_3, evaluated at a given value of developed bending moment, M_o as shown in equations (4) and (5) below.

(4) $\theta(M_o)$ = observed slope change = $\theta_1(M_o) + \theta_2(M_o) - \theta_3(M_o)$

where: $\theta(M_o)$ indicates that θ is a function of the developed moment, M_o , in the joint. Equivalently, θ can be thought of as a function of R, the radius of curvature of the bar, because

$$M_o = \frac{E_s I}{R}$$

Expressing M_o in terms of $\frac{1}{R}$, yields Equation (5)

(5) $$\theta \approx \frac{1}{\beta R} + \frac{a}{2R} - \frac{L}{R_c}$$

Estimating Stresses

The warping tests that have been conducted in this study have shown that the foundation bending reaction results in insignificant values of $\theta_3 = \frac{L}{R_c}$. Therefore, the term $-\frac{L}{R_c}$ may be dropped from Equation (5).

(6) $$\theta \approx \frac{1}{\beta R} + \frac{a}{2R}$$

The resulting expression (6) relates joint face warping rotation to the bar curvature in the joint and the joint opening, a. Therefore, if the warping rotation, θ, and the joint opening, a, are known, it is possible to estimate the radius of curvature of the bar in the joint using formula (6). The

estimated value of $\frac{1}{R}$ can then be used to compute the bar bending stresses in the joint (Equation 7).

$$(7)\quad S_b = \text{Bending strain} \times E_s = \left(\frac{y}{R}\right)E_s = \frac{2\theta\beta}{(2 + a\beta)}\, yE_s$$

where: y is the distance of stressed fibre from neutral axis of bar, and E_s equals Young's modulus of elasticity of the dowel.

Making further use of the approximate foundation theory (2), (3), the maximum concrete bearing stress under the bar, S_c can be estimated.

$$(8)\quad S_c = \frac{G}{2\beta^2}\,\frac{1}{R}, \quad \text{where } G = \frac{4\beta^4 E_s I}{d} \text{ and } d = \text{outside diam of dowel.}$$

Substituting for G in (8) gives an expression for S_c in terms of β.

$$(9)\quad S_c = \frac{2\beta^2 E_s I}{d}\left(\frac{1}{R}\right)$$

APPENDIX B-2

DETERMINING β FROM MATERIAL PROPERTIES OF CONCRETE SUPPORT

Biot (5) has investigated the bending of an elastic beam supported on a three-dimensional elastic foundation (elastic half-space). He has suggested how his results may be incorporated in the elementary one-dimensional foundation formulas (Elastic Foundation Formulation) (2). The suggested procedure consists of equating the maximum moments derived from the approximate theory and the three-dimensional solution which results in an equation for β . The expression equation (1) below, gives β in terms of the material constants of the foundation and known properties of the beam.

$$(1) \quad \beta = .75 \left(\frac{1}{C}\right)\left(\frac{d}{2c}\right)^{.831}$$

$$\text{where } c = \left[2C \ (1-\nu^2) \ \frac{E_b}{E_c} \ \frac{I}{d}\right]^{\frac{1}{3}}$$

E_b = Young's Modulus of beam; I and d are the moment of inertia and depth of the beam; and E_c and ν are, respectively, Young's Modulus and Poisson's Ratio of the foundation. C is a parameter which reflects the stress distribution that exists across any transverse cross-section under the beam.

For the purpose of this analysis, C will be taken to equal 1.13. This is equivalent to assuming the bearing stress to be uniform across the width of the beam at any given transverse section (5).

The material constants, E_c and ν , were determined approximately for the concrete used in test beam No. 3. One concrete cylinder, 4 in. in diameter and 8 in. long, was available for this testing. Two longitudinal strain gages were placed on the cylinder--one gage having a 6-in. gage length and the other, a 3/4-in. gage length. One 6-in. gage was mounted on the circumference at the mid-section of the cylinder. The cylinder was

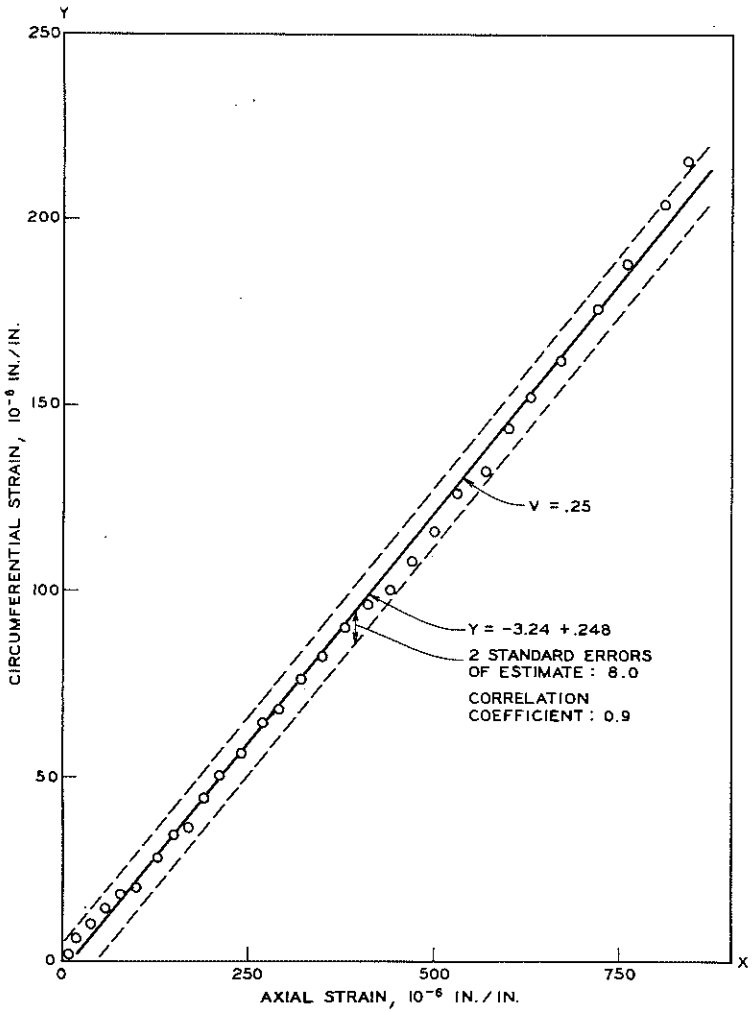

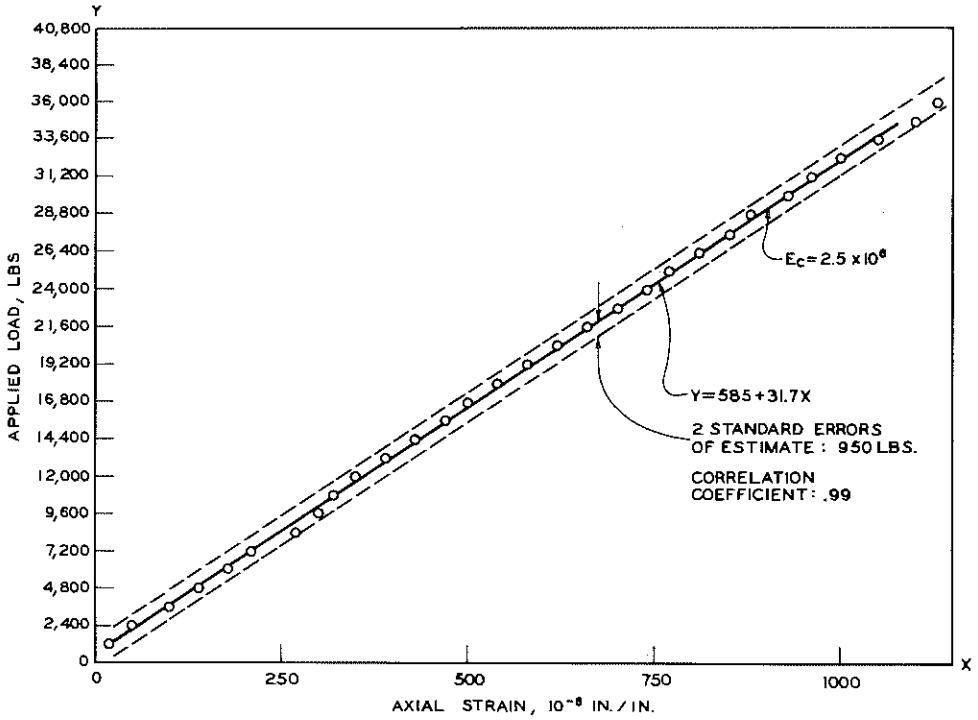

Figure 11. Data plots for determining the material constants E_c and ν.

loaded uniaxially in compression, and the loads applied, and strains measured by the three gages were recorded at discrete points in the loading path. Three trials were run with loads from zero to 3600 lbs being applied. An approximate value of E_c was determined from a longitudinal strain versus load plot of the data from the first trial. The value of E_c obtained was 2.5×10^6 psi. Poisson's Ratio was determined from a longitudinal strain versus transverse strain plot of the Trail 1 data, and was found to be .25. Poisson's Ratio for most concrete is found to vary between .15 and .20. The value obtained in this experiment was therefore higher than anticipated. Figure 11 shows the two data plots used for determining E_c and ν.

Using the approximate values of E_c and ν in equation (1) and setting D = 1.25 in., I = .112 in.^{4}, $E_b = 29 \times 10^6$ and C = 1.13, a value of β can be obtained.

Doing this as shown below, a value of β = .31 is obtained:

$$c = \left[2C\,(1-\nu^2)\,\frac{E_b}{E_c}\,\frac{I}{d} \right]^{\frac{1}{3}} = 1.3$$

$$\beta = (.75)\,\frac{1}{c}\left(\frac{d}{2c}\right)^{.831} = .31$$

Comparison of this value with that shown in Table 1 for Sample 3, indicates that the foundation resisted the rotation of the bar more strongly than could have been predicted based on the measured values of E_c and ν. (The value of β computed from the measured warping rotations was 22 percent larger than computed here, using the measured material constants, ν and E_c).

The difference between the β value computed using Biot's method (5) and that obtained from the warping test may be due in part to physical differences that exist between the assumed foundation (5) and the actual foundation that was provided by the concrete test beams. In the computational method used (5), the foundation was considered to be of infinite extent, and a concentrated load was applied to the beam at the mid point of the foundation. However, in the warping test, the foundation ended at the point

where the bar bending moment was applied. Now if the foundation theory (2) used was not just approximating, β obtained in either case should be the same. This is because the two foundation support conditions are just different boundary value problems and should be governed by the same physical constant if the theory used is valid. However, the theory (2) is only approximately correct and, therefore, different values of β resulted.

If the dowel had been supported on a large concrete block and loaded at the middle, the resulting apparent value of β would be expected to agree with the value computed using the material constants, E_c and ν. The reason for this is that Biot's Method (5) of computing β was derived by equating the approximate foundation formulation (2) to the theoretically correct three-dimensional elastic solution of this particular boundary value problem.

The accuracies of E_c and ν, of course, are also suspect because only one concrete cylinder was tested and because the strain gage lengths used were not optimum. The experimental procedure could be improved in future applications by using larger test cylinders (6 in. diam by 12 in. long), instrumented with several 4-inch strain gages. More than one cylinder should be tested per batch of concrete as well.

APPENDIX B-3

DIRECT DETERMINATION OF β FROM CONCENTRATED LOAD EXPERIMENTS
(See Reference (6))

According to the one-dimensional elastic foundation theory (3), β is expressed by:

$$(1) \quad \beta = \left(\frac{Gd}{4E_S I}\right)^{\frac{1}{4}}$$

where:
- G = Modulus of support of the concrete mass
- d = Outside diameter of dowel
- E_S = Modulus of elasticity of steel dowel (29×10^6 psi)
- I = Moment of inertia of the dowel

Also according to the one-dimensional theory, the vertical displacement of the dowel being subjected to a vertical load near the face of the concrete mass is expressed by:

$$(2) \quad Y_o = \text{displacement} = \left(\frac{P}{2\beta^3 E_S I}\right)\left(1 + \beta x\right)$$

where:
- P = Vertical load applied to the dowel in the joint
- x = Eccentricity of the vertical load from face of concrete mass

It is possible to derive an expression for β in terms P and Y_o from the two expressions given. Substituting Equation (1) into (2) and simplifying the results leads to the following implicit expression for β .

$$(3) \quad \beta = \left(\frac{P\ (1 + x\ \beta)}{2\ Y_o\ E_S I}\right)^{\frac{1}{3}}$$

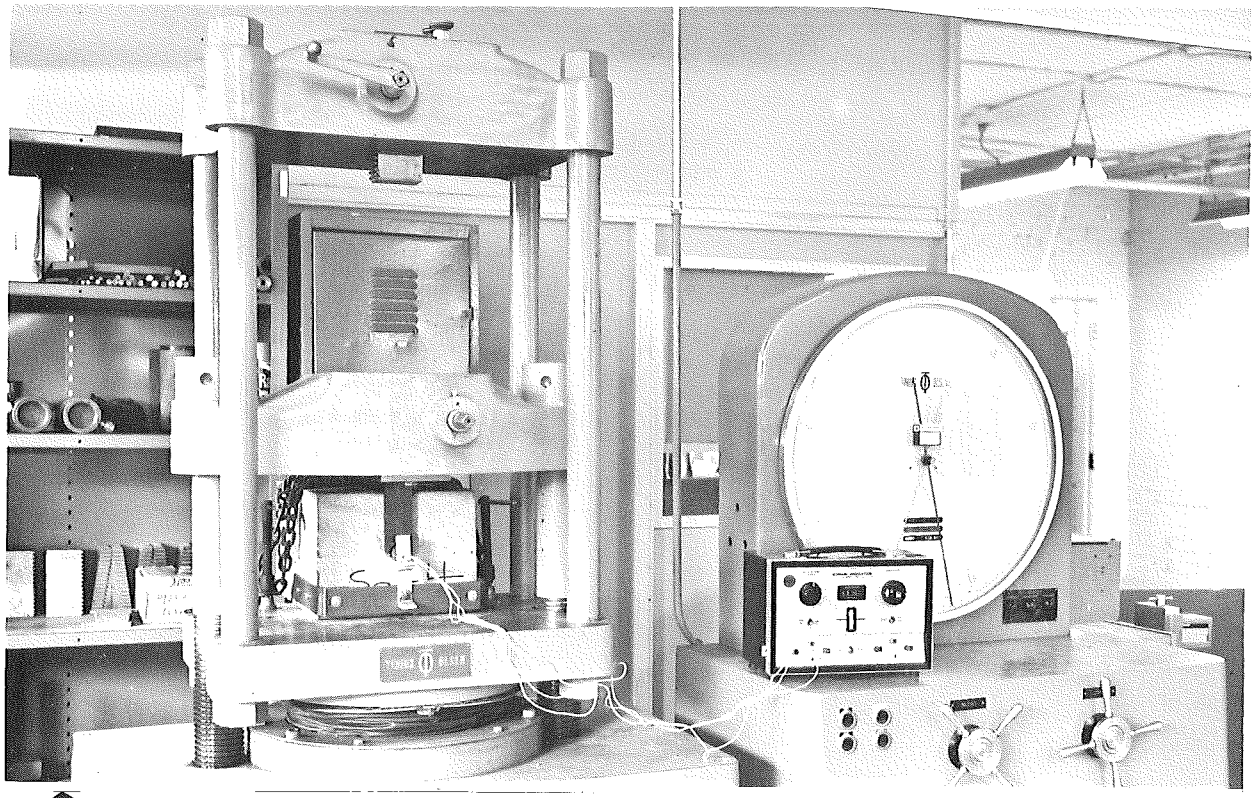

Testing apparatus and block sample.

Cantilever deflectomer device used for measuring vertical dowel displacement relative to test block.

Loading bar in contact with dowel stub protruding from test block.

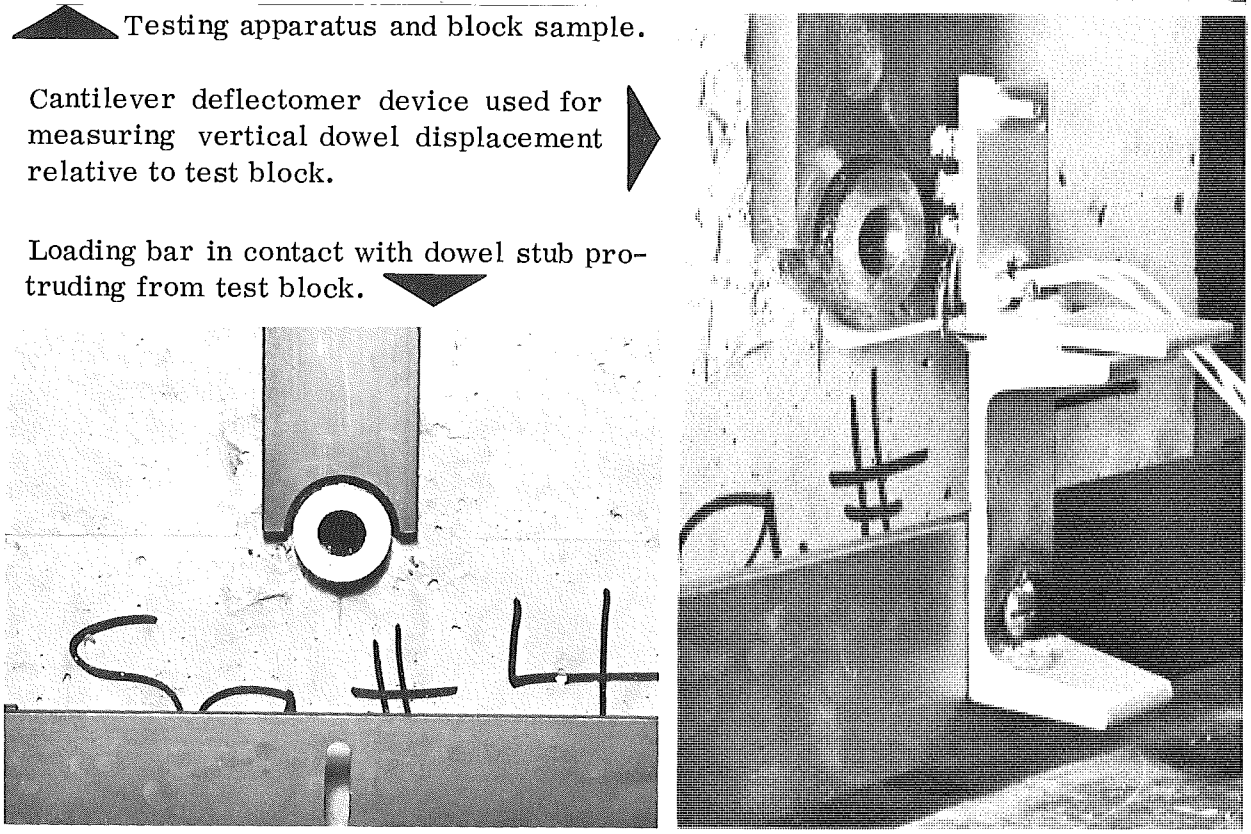

Figure 12. Direct load β test apparatus.

For small values of x, ($x \beta << 1$) this formula reduces to an approximate explicit expression of β, if the term $x \beta$ is neglected.

$$(4) \quad \beta = \left(\frac{P}{2 Y_o E_s I} \right)^{\frac{1}{3}}$$

The following experimental procedure was used in attempting to determine β for the four beam samples by utilizing Equation (4).

1. The dowel bar in each test beam was cut at the joint with a band saw separating each beam into two blocks. The cut was made near one concrete face of the beam sample so that one block in each sample had a short stub of the bar extending through its surface.

2. One block from each sample was loaded in the universal testing machine. The load was applied through a flat loading bar onto the dowel bar stub projecting from the face of each block (Figure 12).

3. A deflectometer consisting of a cantilever device with a strain gage attached to it was used to measure the movement of the bar relative to the concrete block. A material frame of reference was established for this measurement by mounting the deflectometer to a steel frame which was directly bolted to the concrete block (Figure 12).

4. Discrete values of applied load, P, and dowel displacement, Y_o, relative to the block foundation were recorded for each test beam. The loading proceeded from 0 to 4,000 lbs and was repeated three times for each sample.

5. Y_o versus P curves were plotted from the data. Figure 13 shows the three curves obtained for test beam No. 3. According to Equation (4), the ratio $\frac{P}{Y_o}$ should have remained constant during the loading. However, the graphs illustrate that the ratio $\frac{P}{Y_o}$ varied as the load, P, was increased. Therefore it was not possible to calculate β from the test data using Equation (4).

In summary, the test results of the concentrated load experiment indicate that it is not possible to determine β from such tests. The relationship between P and Y_o obtained from these tests was nonlinear.

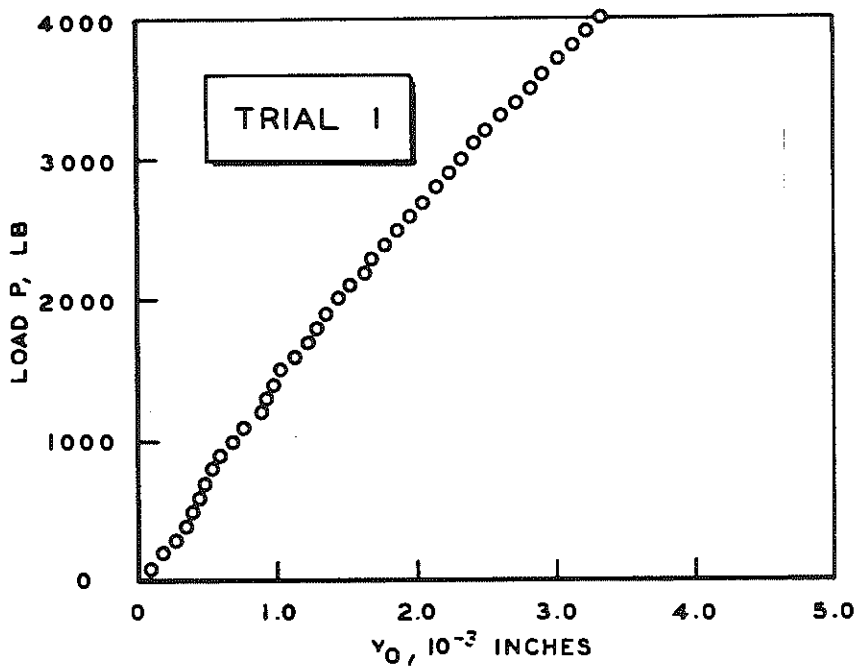

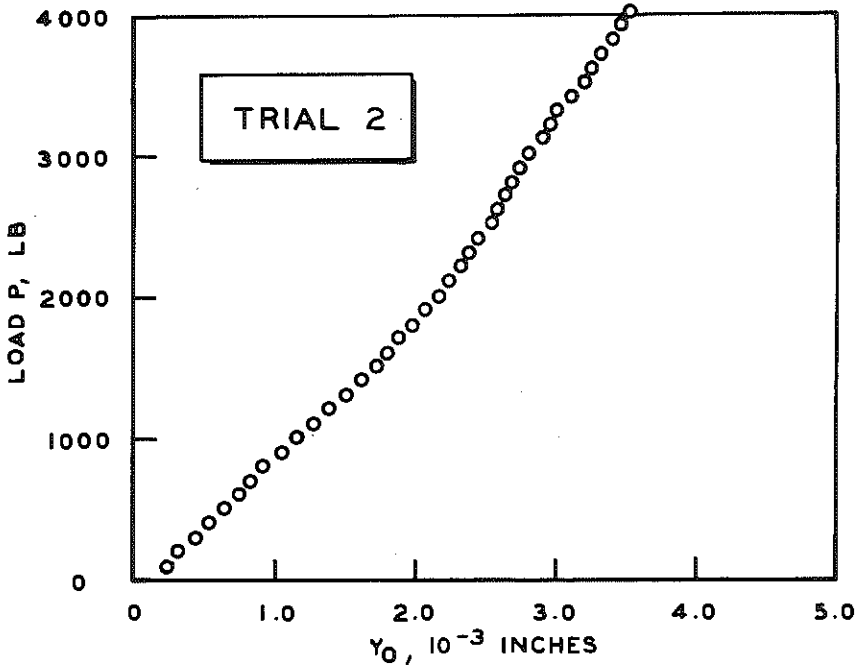

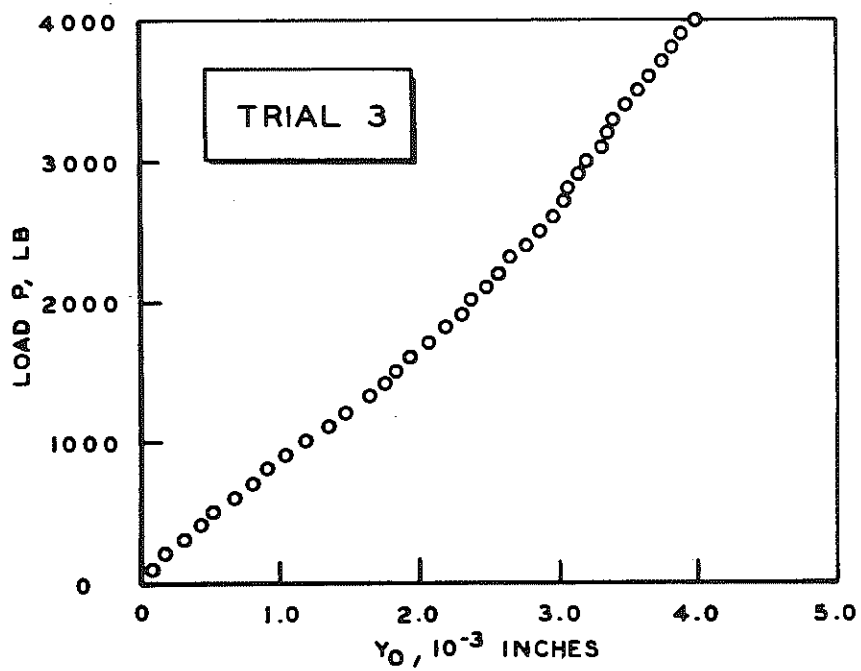

Figure 13. Y_O versus P curves plotted from data obtained from beam No. 3.

BIBLIOGRAPHY

1. Harr, M. E., and Leonards, G. A., "Warping Stresses and Deflections in Concrete Pavements," Highway Research Board, Vol. 38, 1959, pp 286-320 and Vol. 39, pp 157-172.

2. Timoshenko, S., and Lessels, J. M., APPLIED ELASTICITY, Westinghouse Technical Night School Press, 1925, pp 131-141.

3. Friberg, B. F., "Load and Deflection Characteristics of Dowels in Transverse Joints of Concrete Pavements," American Society of Civil Engineering Transactions, Vol. 105, 1940, pp 1078-1080.

4. "Structural Design Considerations for Pavement Joints," Subcommittee 111, ACI Committee 325, Journal of the American Concrete Institute, Vol. 28, July, 1956, pp 1-28.

5. Biot, M. A., "Bending of an Infinite Beam on an Elastic Foundation," Journal of Applied Mechanics, Transactions, American Society of Mechanical Engineers, Vol. 59, 1937, pp A1-A7.

6. Cudney, G. R., and Behr, R. D., "Determination of the Modulus of Concrete Support, G, For the Design of Dowels in Transverse Pavement Joints," Michigan Department of State Highways, July, 1955, Report No. 233.